Journal of Power Sources 373 (2018) 95–102

Contents lists available at ScienceDirect

Journal of Power Sources

journal homepage: www.elsevier.com/locate/jpowsour

A thermally regenerative ammonia battery with carbon-silver electrodes for converting low-grade waste heat to electricity

Mohammad Rahimi[a], Taeyoung Kim[b], Christopher A. Gorski[b], Bruce E. Logan[b,*]

[a] Department of Chemical Engineering, The Pennsylvania State University, University Park, PA 16802, USA
[b] Department of Civil and Environmental Engineering, The Pennsylvania State University, University Park, PA 16802, USA

HIGHLIGHTS

- A battery based on a ligand and silver salts was developed to produce electricity.
- Carbon paper or cloth loaded with silver particles were used as the electrode.
- Silver battery showed a higher performance compared to copper battery.
- The power density of silver battery was enhanced by up to 64%.
- The silver battery produced a stable power over a hundred charge/discharge cycles.

GRAPHICAL ABSTRACT

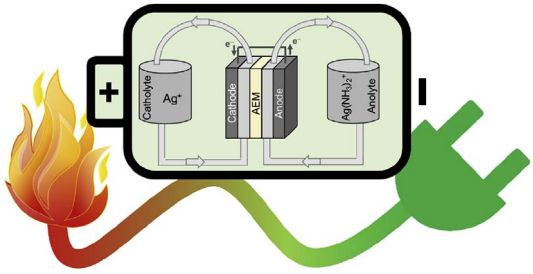

ARTICLE INFO

Keywords:
Energy conversion
Waste heat
Thermally regenerative battery
Rechargeable battery

ABSTRACT

Thermally regenerative ammonia batteries (TRABs) have shown great promise as a method to convert low-grade waste heat into electrical power, with power densities an order of magnitude higher than other approaches. However, previous TRABs based on copper electrodes suffered from unbalanced anode dissolution and cathode deposition rates during discharging cycles, limiting practical applications. To produce a TRAB with stable and reversible electrode reactions over many cycles, inert carbon electrodes were used with silver salts. In continuous flow tests, power production was stable over 100 discharging cycles, demonstrating excellent reversibility. Power densities were 23 W m^{-2}-electrode area in batch tests, which was 64% higher than that produced in parallel tests using copper electrodes, and 30 W m^{-2} (net energy density of 490 Wh m^{-3}-anolyte) in continuous flow tests. While this battery requires the use a precious metal, an initial economic analysis of the system showed that the cost of the materials relative to energy production was $220 per MWh, which is competitive with energy production from other non-fossil fuel sources. A substantial reduction in costs could be obtained by developing less expensive anion exchange membranes.

1. Introduction

Low-grade waste heat (temperature < 130 °C) generated by industrial plants and geothermal and solar-based systems is estimated to be major sustainable energy source for the future [1–3]. Low-grade waste heat generated at industrial plants in U.S.A contains approximately half of the current energy demand of this country (2.9×10^{13} kWh in 2013) [4], and recovering even a fraction of this energy would be a major step towards developing a more sustainable energy infrastructure [5–9]. Technologies to convert low-grade waste heat to electricity must produce high power densities and be efficient, scalable, and cost-effective [1,10], but so far no approach has met all

* Corresponding author.
E-mail address: blogan@psu.edu (B.E. Logan).

http://dx.doi.org/10.1016/j.jpowsour.2017.10.089
Received 27 June 2017; Received in revised form 19 October 2017; Accepted 30 October 2017

these goals. For example, solid-state thermoelectric devices based on p- and n-type semiconductor materials have high material costs, lack the capacity for energy storage, and have relatively low power densities [1,11,12]. Liquid-based thermoelectrochemical cells (TECs) could potentially provide a more cost effective and scalable approach, but power densities have generally been in the range of only 0.5–6.6 W m^{-2} [13–15]. One TEC produced 12 W m^{-2}, with an inter-electrode temperature difference of 81 °C, but the efficiency relative to the Carnot cycle was only 0.4% [16], which was low compared to other approaches (efficiencies of 1.4–4.0%) [13–15]. As a result of these relatively low power densities and thermal-electrical inefficiencies, solid state and TECs have not yet been commercialized [17].

Recently, a new approach for converting low-grade waste heat to electricity, called a thermally regenerative ammonia battery (TRAB), was shown to produce significantly higher power densities than TECs or other approaches [18]. A flow TRAB with copper electrodes and salts produced a maximum power density of ~25 W m^{-2} (normalized to a single electrode area), with an estimated Carnot thermal-electrical conversion efficiency of 5% [19]. TRABs generate electrical power from electrochemical potentials produced by adding a ligand to one electrolyte chamber, with the two chambers separated by a membrane. The first TRAB used copper mesh electrodes and a copper nitrate electrolyte (Cu-TRAB), with ammonia as the ligand [18]. When ammonia is added to one electrolyte chamber it becomes the anode chamber, due to formation of a copper ammine complex. When the potential difference between the electrodes is discharged, the anode undergoes oxidative dissolution, and aqueous copper ions are reductively deposited on the cathode (Eqn. S1, S2). After discharging, the ammonia is separated from the anolyte using conventional separation technologies, such as distillation or air stripping, using low-grade waste heat [18,20]. The separated ammonia is then added to the former cathode chamber, so that the function of the chambers is switched, ideally achieving a closed-loop cycle with no net loss of copper form the electrode. In order to provide stable operation over many cycles, metal deposition on the cathode must be balanced with metal removal in the next cycle. However, the conversion of the copper anode into current in the Cu-TRAB was only 35% (i.e., approximately three times as much copper dissolves from the electrode as would be expected) [18–20]. This irreversible loss of copper from the anode limited the number of possible cycles using this copper and ammonia-ligand system. The use of an alternative ligand (ethylenediamine) reduced, but did not eliminate, irreversible losses of copper from the anode [21].

A new type of TRAB was developed here based on using carbon electrodes and solutions containing dissolved silver to avoid losses of the metal to reaction with the electrolyte and enable fully reversible charging cycles. The open circuit voltage using silver (0.45 V) is very similar to that of copper (0.44 V), but the anode and cathode potentials are much more positive than those for copper, with half-cell reactions of:

$$\text{Cathode: } Ag^{+}_{(aq)} + e^{-} \rightarrow Ag_{(s)} \qquad E^0 = +0.80\ V \tag{1}$$

$$\text{Anode: } Ag_{(s)} + 2\,NH_{3\,(aq)} \rightarrow Ag(NH_3)^{+}_{2\,(aq)} + e^{-} \qquad E^0 = +0.37\ V \tag{2}$$

where E^0 is the standard reduction potential (vs. SHE) [22]. For copper, the cathode E^0 value is +0.34 V and the anode E^0 value is −0.04 V vs. SHE (Eqn. S1, S2) [23]. To demonstrate the feasibility of sliver-based TRAB (Ag-TRAB), power production was examined in single cycle tests (fed batch conditions) using silver nitrate solutions and carbon paper electrodes, and compared to power generated using a Cu-TRAB containing copper mesh electrodes and a copper nitrate solution. Power production was then examined in a continuous flow system with carbon paper or carbon cloth anodes, with the reversibility and stability of the carbon cloth electrodes studied by cycling the battery one hundred times. The morphology of the silver electrodeposited on the carbon electrodes was examined using a scanning electron microscope (SEM), and the cost of electricity produced was evaluated on the basis of the cost of the materials used in the continuous flow system.

2. Materials and methods

2.1. Silver electrodeposited electrode preparation and characterization

Commercially available carbon cloth and paper (AvCarb Material Solutions) were treated to improve surface hydrophilicity and reaction with silver, by soaking overnight at room temperature in a mixed solution of concentrated sulfuric and nitric acids (v:v = 3:1) [24,25]. The materials were then thoroughly rinsed and then stored in DI water prior to use. Silver was electrodeposited onto the carbon electrodes (cloth or paper) in a cubic reactor (4 cm long and 3 cm in diameter) with platinum mesh (AMETEK Inc.) as the counter electrode. The electrolyte was mixed using a magnetic stirrer (6.4 × 15.9 mm; VWR) at 500 rpm. A current density of 7 mA cm^{-2} was applied for 60 min to deposit silver onto the carbon electrodes. Based on the amount of silver deposited on the carbon materials (calculated by measuring the weight of the substrate before and after the electrodeposition), the coulombic efficiencies were > 90% for silver deposition ($Ag^{+} + e^{-} \rightarrow Ag^{0}$) (Table S1). The electrolyte was 0.1 M $AgNO_3$ with a 5 M NH_4NO_3.

Silver deposited electrodes were examined using scanning electron microscopy (SEM; NanoSEM 630, FEI, Hillsboro, OR) to observe the morphology and size of the silver particles. Energy-dispersive X-ray spectra (EDS; NanoSEM 630, FEI, Hillsboro, OR) were used to identify composition of the particles formed on the carbon substrate.

2.2. TRAB construction and operation

Power densities and anodic coulombic efficiencies of the Ag-TRAB were first evaluated in a fixed volume battery (no flow conditions) that had sufficient room for reference electrodes to monitor electrode potentials, constructed as previously described [23,26]. Briefly, the cell consisted of a cathode and an anode chamber, each 4 cm long and 3 cm in diameter, separated by an anion exchange membrane (AEM; Selemion AMV, Asashi Glass, Japan), producing an electrode area per volume of reactor of 25 m^2 m^{-3}. Two silver electrodeposited carbon papers were used as the electrodes, with each electrode placed at the end of the reactor. To monitor the electrode potentials, two Ag/AgCl reference electrodes (+0.211 V vs. SHE; RE-5B; BASi) were inserted 1 cm away from each electrode (Fig. S1). The power production and coulombic efficiency of Ag-TRAB were also compared to those of the Cu-TRAB. The same reactor configuration was used for the Cu-TRAB but the electrodes were copper mesh (50 × 50 mesh; McMaster-Carr, OH), consistent with previous tests [21,23].

The remaining tests were conducted using a compact, custom-built flow cell with a design similar to our previous tests [27,28]. The flow cell consisted of two thin circular channels (diameter = 3 cm; thickness = ~100 μm) separated by an AEM that were fed with either the electrolyte containing ammonia (anolyte) or plain electrolyte, with an electrode packing density of 10,000 m^2 m^{-3}. The electrodeposited silver-carbon electrodes were placed in each channel, and graphite foil behind the electrodes was used as a current collector. The symmetrical cell was sealed using two end plates (Fig. 1).

The electrolytes were prepared using 0.1 M of either $AgNO_3$ (Sigma-Aldrich; Ag-TRAB) or $Cu(NO_3)_2$ (Sigma-Aldrich; Cu-TRAB) with 5 M NH_4NO_3 as the supporting electrolyte to increase conductivity. Ammonium hydroxide (2 M final concentration; 5 N solution, Sigma-Aldrich) was added only to one chamber (anolyte) to form the metal ammonia complex and create a potential difference between the anode and cathode chambers. The electrolyte composition was chosen based on the optimum values previously reported [18].

2.3. Cell performance evaluation

Polarization tests were performed using a potentiostat (model

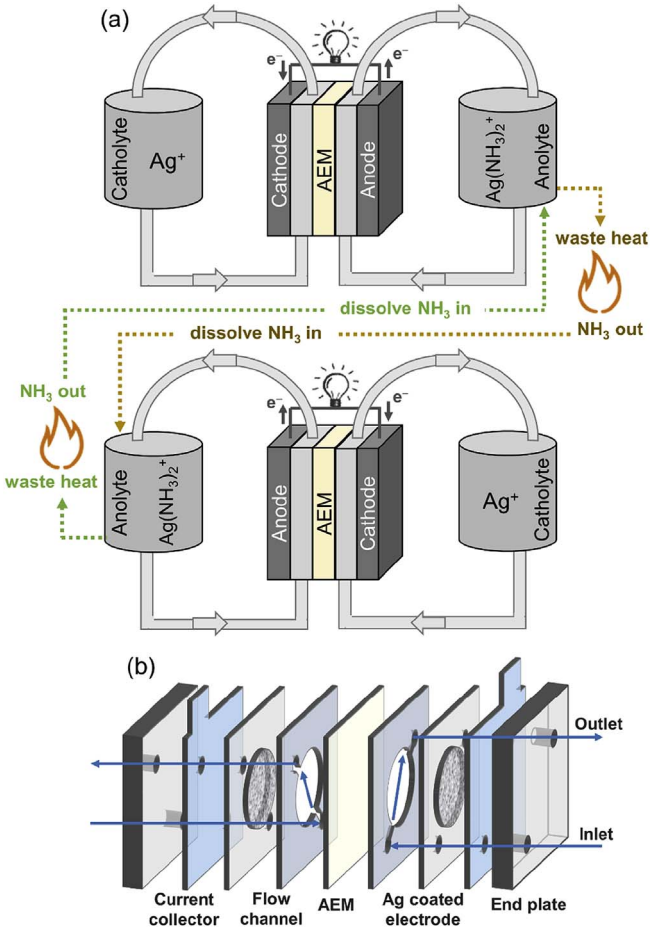

Fig. 1. (a) Schematic of the flow silver TRAB for converting low-grade waste heat to electricity. Power was produced using two identical carbon-based Ag electrodeposited electrodes in the cell while flowing the catholyte (0.1 M $AgNO_3$, 5 M NH_4NO_3) and the anolyte (0.1 M $AgNO_3$, 5 M NH_4NO_3 and 2 M NH_4OH) through two channels separated by an anion-exchange membrane (AEM). After the cell discharge, ammonia is separated from the anolyte using a conventional distillation with low-grade waste heat, and then added to the other electrolyte for the sequel discharge cycle. By repeating the cycles, low-grade waste heat is converted to electricity. (b) Detailed diagram indicating components the symmetrical flow cell.

1470E, Solatron Analytical, Hampshire, England) to measure the cell voltage (U, V), and each electrode potential (batch cell only), at room temperature (23 °C). For both batch and flow cells, external resistances were switched every 2 min from open circuit to a minimum of 1.4 Ω. Both current density ($i = U/RA$), and power density ($P = U^2/RA$, W m^{-2}) were normalized to a single electrode projected surface area ($A = 7$ cm^2), where i (A m^{-2}) is the current density and R (Ω) the external resistance. The energy density, normalized to the total electrolyte volume of the flow cell (E, Wh m^{-3}), was calculated as $E = \int U I\, dt/V$, where I (A) is the current, t is cycle time, and V (m^3) is the total volume.

The net power density produced by the stack (P_{net}, W m^{-2}) was obtained by subtracting the hydrodynamic power loss (P_{hydro}) from the electrical power produced. Hydrodynamic power losses (P_{hydro}, W m^{-2}; normalized to the electrode area) from flow through the electrolyte chambers were calculated based on the pressure drop according to [29,30]:

$$P_{hydro} = \frac{2Q_f \Delta P_t}{A} \tag{3}$$

where Q_f (m^3 s^{-1}) is the flow rate, ΔP_t (Pa) the theoretical pressure drop, and A (m^2) the electrode surface. The theoretical pressure drop is given by Ref. [31]:

$$\Delta P_t = \frac{12\mu L Q_f}{d^3} \tag{4}$$

where μ (Pa s) is the dynamic viscosity of water, L (m) the length of the reactor, and d (m) the flow channel thickness.

Coulombic efficiencies were calculated to evaluate the reversibility of silver or copper deposition or dissolution from the electrodes. The cathodic coulombic efficiency (*CCE, %*) was calculated as the ratio between actual transferred charge and the theoretical amount of charge based on the change in the mass change of the electrode:

$$CCE = \frac{(m_{f,c} - m_{0,c})nF}{Q\,M} \times 100 \tag{5}$$

where $m_{0,c}$ and $m_{f,c}$ (g) are electrode masses of cathode before and after the discharge test, n (Cu, $n = 2$; Ag, $n = 1$) is the number of electron transferred in the reduction reaction, F (96485 C mol^{-1}) is the Faraday's constant, Q ($Q = \int I\, dt_s$, C) is the total charge transferred, and M is the molecular weight of the metal (Cu, 63.55 g mol^{-1}; Ag, 107.87 g mol^{-1}). Similarly, the anodic coulombic efficiency (*ACE*) was calculated as:

$$ACE = \frac{Q\,M}{(m_{0,a} - m_{f,a})n\,F} \times 100 \tag{6}$$

where $m_{0,a}$ and $m_{f,a}$ (g) are electrode masses of anode before and after the discharge test, measured using an analytical balance with a precision of 0.0001 g. The Coulombic efficiency refers to the ratio (as a percentage) of the mass of metal deposited or removed relative to the integral of the generated current. For example, if more mass is lost than charge transferred through the circuit, then mass was lost to side reactions that did not generate current. If the mass lost from the anode is not equal as the mass gained when it is a cathode, the electrode cycles irreversibly. For electrode cyclability to be reversible, the Coulombic efficiency must be 100%.

Cyclic voltammetry (CV) was used to further study the factors that could explain the coulombic efficiency of anode. CV studies of the anolyte of both Ag-TRAB and Cu-TRAB were performed using a potentiostat (VMP3, BioLogic) using a glassy carbon working electrode, a platinum wire counter electrode, and an Ag/AgCl reference electrode. CVs were run at the potential range of −0.6 V to 0.6 V with a scan rate of 25 mV s^{-1} [21].

Electrochemical impedance spectroscopy (EIS; VMP3, Bio-Logic) was used to quantify the different components (ohmic and reaction) of the overall resistance. All EIS experiments were measured over a frequency range of 100 kHz to 0.1 Hz with a sinusoidal amplitude of 10 mV. The EIS spectra were fitted into a simplified Randles equivalent circuit, as done in for the previous TRAB analysis [18], in order to calculate the resistance of each component (Fig. S2).

The charge/discharge reversibility of flow Ag-TRAB with a carbon cloth based silver-electrodeposited electrodes was tested over a hundred successive cycles by switching the flow path (switching the electrode function) every 3 min with a fixed external resistance of 10 Ω. The same catholyte (0.1 M $AgNO_3$, 5 M NH_4NO_3) and anolyte (0.1 M $AgNO_3$, 5 M NH_4NO_3, 2 M NH_4OH) were used, and the cell potential was recorded every 30 s during the experiment.

Discharge energy efficiency (η_d, %) of the flow Ag-TRAB, based on the removal of silver ions from the catholyte through electrochemical deposition onto the cathode, was calculated as:

$$\eta_d = \frac{Q}{C_i V_c F} \times 100 \tag{7}$$

where C_i (0.1 M) is the initial concentration of silver ion, and V_c (0.01 L) is the volume of the catholyte. A η_d value of 100% indicates that all the chemical energy related to the presence of silver ions stored in the cell was converted to electrical power.

Thermal energy efficiency (η_t) was calculated as the ratio between the net energy production of the battery and the required heat energy

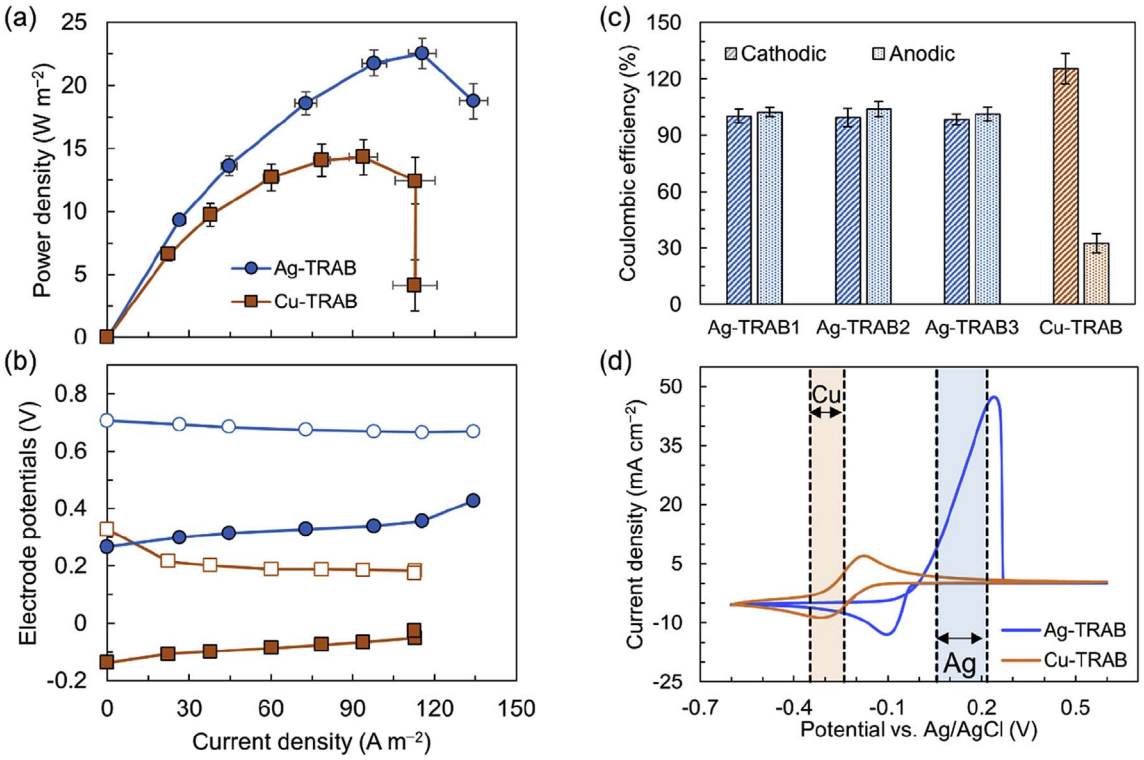

Fig. 2. Comparison of (a) power densities, (b) cathode (open symbols) and anode (filled symbols) potentials, (c) coulombic efficiencies, and (d) cyclic voltammetry (scan rate of 25 mV s^{-1}) of a silver TRAB (Ag-TRAB) and a copper TRAB (Cu-TRAB). The highlighted area in part d indicates the potential range of the anode for the silver and copper TRABs.

for anolyte regeneration by separation of ammonia. Based on a simulation using Aspen HYSYS® (version 8.6), the energy requirement for ammonia separation was 134 kWh m^{-3}-anloyte, based on a conventional distillation column with a reboiler temperature of 60 °C, condenser temperature of 43 °C, and an inlet stream temperature of 27 °C [20]. In order to compare the energy efficiencies of this system with previous thermoelectrochemical cells, thermal efficiency was also reported relative to the Carnot efficiency, by dividing the actual thermal efficiency (η_t) by the Carnot efficiency. Carnot efficiency (η_c) was calculated as $\eta_c = (T_H - T_C)/T_H$, where T_H is the reboiler temperature (333 K) and T_C is the temperature of the distillation inlet stream (300 K).

3. Results and discussion

3.1. Power production and electrode potentials

The maximum power density of the Ag-TRAB was 23 W m^{-2}, at a current density of 115 A m^{-2}, based on polarization tests using the fed-batch battery (Fig. 2a). This power density was 64% higher than that obtained here using a copper-based TRAB of 14 W m^{-2}. An analysis of components of the internal resistance using EIS indicated that the Ag-TRAB had a higher ohmic resistance (2.45 Ω) than the Cu-TRAB (2.22 Ω), but less reaction resistance (Ag-TRAB, 0.37 Ω; Cu-TRAB, 1.66 Ω), and therefore a smaller total resistance (Fig. S3). Thus, the lower reaction resistance of the Ag-TRAB was the main reason for the improved power.

The open circuit voltage of silver-based TRAB was 0.45 V, with a cathode potential of 0.71 V vs. SHE and an anode potential of 0.27 V vs. SHE. The open circuit potential of Ag-TRAB was very similar to that of Cu-TRAB (0.44 V), but the anode and cathode potentials were much higher (Cu-TRAB, +0.33 V for cathode, −0.14 V for anode; Fig. 2b). This shift to a higher potential might change the electrochemical behavior of species in both catholyte and anolyte.

Coulombic efficiencies (CCE and ACE) were calculated to study electrode reversibility. The CCE and ACE of Ag-TRAB were very similar and close to 100% over three successive cycles (Fig. 2c). This showed that equal masses of silver were dissolved from the anode and deposited on cathode, producing conditions needed for a reversible system. In contrast, the Cu-TRAB had a very low ACE of 35%, consistent with previous results [18,20], indicating a large loss of copper due to its dissolution without current generation.

Cyclic voltammetry (CV) was used to further understand why the coulombic efficiencies of the anode and cathode were effectively 100%. The anode potential range of the Ag-TRAB (highlighted blue area; Fig. 2d) did not cover the silver ammine complex reduction peak, indicating that the operation range for the anode potential would have an insignificant loss of silver with non-current producing reactions. Thus, anode dissolution was due to favorable current production by the reaction: $Ag + 2\ NH_3 \rightarrow Ag(NH_3)_2^+ + e^-$. However, for the copper-based TRAB, the anode potential occurred at a potential favorable for the reduction of copper with the ammine complex in solution (Eqn. S (3)), and thus substantial copper loss resulted in metal dissolution not associated with current production, leading to a low ACE [21]. The different anode potentials relative to the non-current producing reaction of the solid metal phase with the solution thus explained the significant differences in ACEs between silver and copper TRABs. Further information on the CVs was provided in Section 1 in the Supporting Information.

3.2. A silver-based continuous flow TRAB

3.2.1. Electrode characterization

Silver particles were observed using SEM to be uniformly distributed with no particle agglomeration on both carbon cloth and paper. The silver particle size was observed to be 21 ± 8 μm for carbon cloth and 32 ± 10 μm for carbon paper. The carbon substrates also showed no deformation and physical degradation, confirming the physical stability of carbon cloth and paper electrodes during the silver electrodeposition process (Fig. 3a and b; Fig. 4S). EDS analysis of the

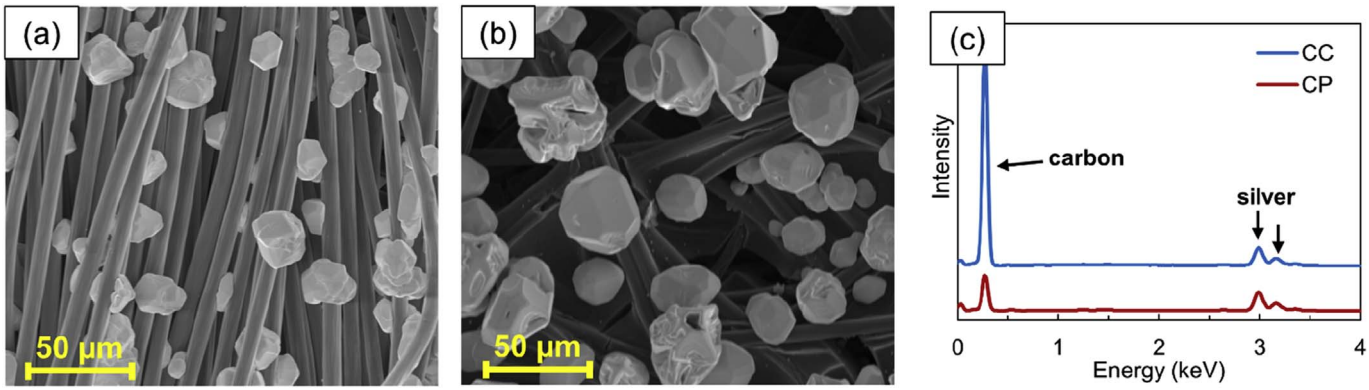

Fig. 3. SEM images of the silver electrodeposited electrodes with (a) carbon cloth (CC) and (b) carbon paper (CP) substrates. The corresponding EDS spectrum (c) indicates a successful deposition of silver on both carbon cloth and carbon paper substrates.

samples confirmed that the particles were metallic silver (Fig. 3c).

3.2.2. Power production at different flow rates

Polarization tests were used to evaluate the maximum power densities at various flow rates in the continuous flow Ag-TRAB using carbon cloth or carbon paper electrodes (Fig. 4). For both carbon substrates, the maximum power production increased with flow rate, likely due to a reduction in the concentration boundary layer as a result of the enhanced mass transfer at higher flow rates [19,32]. For example, the maximum power density increased from 24 W m^{-2} at a flow rate of 0.5 mL min^{-1} to 31 W m^{-2} at a flow rate of 6 mL min^{-1} for a cell with carbon cloth electrodes. However, the energy losses for pumping the electrolyte through the flow channels (i.e., hydrodynamic power loss) also increased concurrently with flow rate [29,31]. As a result, the net power production, which was calculated by subtracting the hydrodynamic power loss from the power production, decreased for the higher flow rates, with the highest net power production obtained at a flow rate of 2 mL min^{-1} (hydraulic retention time = 2 s) for both carbon cloth (28 W m^{-2}) and paper (24 W m^{-2}) electrodes (Fig. 4).

Based on EIS tests, the reaction resistance (0.08 Ω on average) and total resistance (2.32 Ω on average) were lower with carbon cloth electrodes than carbon paper electrodes (0.13 Ω reaction, and 2.42 Ω total) (Fig. 5). The reduced reaction resistances indicated that the electrochemical oxidation and reduction of silver ions were more favorable on carbon cloth than on carbon paper. The difference between reaction resistances of carbon cloth and paper was likely due to the differences in surface roughness [33,34], pore size distribution [33,35], surface area [33], and hydrophilicity [35]. As observed for the fed batch battery, the lower reaction resistance was the main reason for higher power densities on carbon cloth compared to carbon paper.

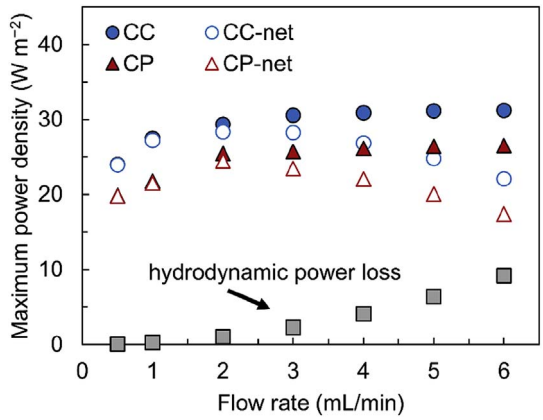

Fig. 4. Maximum power densities of the silver TRAB with Ag electrodeposited electrode on carbon cloth (CC) and carbon paper (CP) substrates at different flow rates with 0.1 M $AgNO_3$, 5 M NH_4NO_3 and 2 M NH_4OH (anode). The open symbols indicate the net power production by subtracting the hydrodynamic power loss (gray symbols) from the power production (filled symbols) at each flow rate.

3.2.3. Energy production of the flow Ag-TRAB

The energy density of a flow Ag-TRAB was obtained by recycling each electrolyte (10 mL), at different flow rates, with the external resistance that produced the maximum power density in polarization tests (2.5 Ω). Total energy production was enhanced by increasing the flow rate, owing to the lower transfer rate of hydroxide ions. The transfer of hydroxide from the alkaline anode chamber (pH = 9.5) to the acidic cathode chamber (pH = 2.3) results in a shift in the NH_4^+/NH_3 acid/base equilibrium towards NH_3 formation in the cathode chamber. This formation of NH_3 in the cathode chamber eventually reduced the consumption of silver ions through an unfavorable chemical reaction ($Ag^+ + 2NH_3 \rightarrow Ag(NH_3)_2^+$) (Figs. S5 and S6) [23]. The formation of $Ag(NH_3)_2^+$ by the chemical reaction in the catholyte does not affect the coulombic efficiencies, but it can reduce the energy densities of the discharge cycles [21,23]. Similar to polarization test results, net energy density was calculated by subtracting the energy to pump the electrolyte from the total energy produced (Fig. 6). The highest net energy densities of 493 Wh m^{-3}-anolyte for carbon cloth and 440 Wh m^{-3}-anolyte for carbon paper were obtained at a flow rate of 2 mL min^{-1}. These energy densities were lower than that previously reported for a flow Cu-TRAB (1260 Wh m^{-3}) [19], but the silver-based reactions were fully reversible while the copper-based reactions were not. The discharge efficiency (net electrical energy captured versus chemical energy in the starting solution) followed the same trend as the energy densities, with the highest efficiencies of 94% (carbon cloth) and 88% (carbon paper) at a flow rate of 2 mL min^{-1}. These discharge efficiencies of the Ag-TRAB were significantly higher than those previously reported for the Cu-TRAB (26%–30%) [18,19,21,23].

Thermal efficiency, defined as the ratio between the produced energy density and the thermal energy for anolyte regeneration, was 0.41% for the Ag-TRAB. The calculated thermal efficiency relative to the Carnot efficiency was 3.8%, which was within the range of 2–5% that previous work estimated was necessary for a heat-to-electricity technology to be commercially viable [36].

3.2.4. Electrode behavior during the cell discharge

The silver electrodeposited electrodes examined using SEM analysis (Fig. 7) showed a uniform distribution of silver particles with no agglomeration after discharging the cell (electrical power production) for 1, 10 and 22 min (the whole discharge). The silver particle sizes increased with discharge times, and no deformation, degradation, and failure of material were observed for the carbon substrates, confirming that only silver particles (and not the carbon substrate) were involved in the reactions during the cell discharge. These showed that the carbon

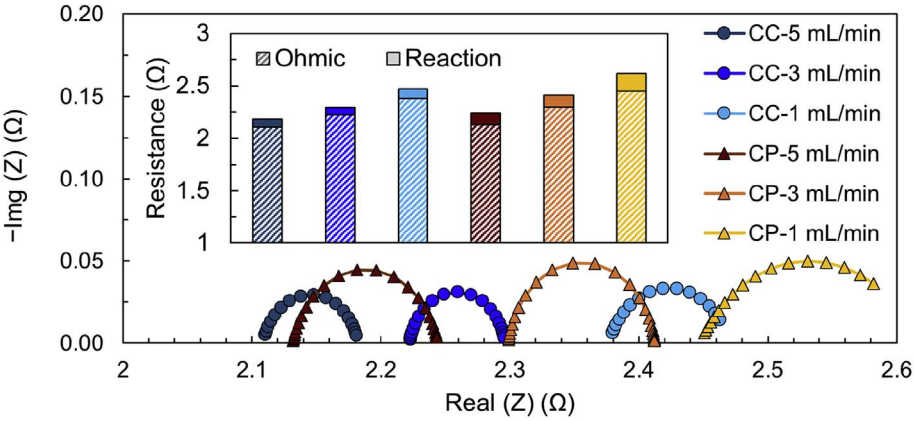

Fig. 5. Nyquist plots of the whole cell impedance for flow silver TRAB with carbon cloth (CC; blues) and carbon paper (CP; reds) Ag electrodeposited electrodes. The inserted figure indicates the components of impedance (ohmic, patterned; reaction, filled) obtained by fitting the Nyquist plots to the equivalent simplified Randles circuit (Fig. S2). The electrolyte was 0.1 M $AgNO_3$, 5 M NH_4NO_3 and 2 M NH_4OH (anode), and different flow rates were investigated (5, 3, 1 mL min^{-1}).

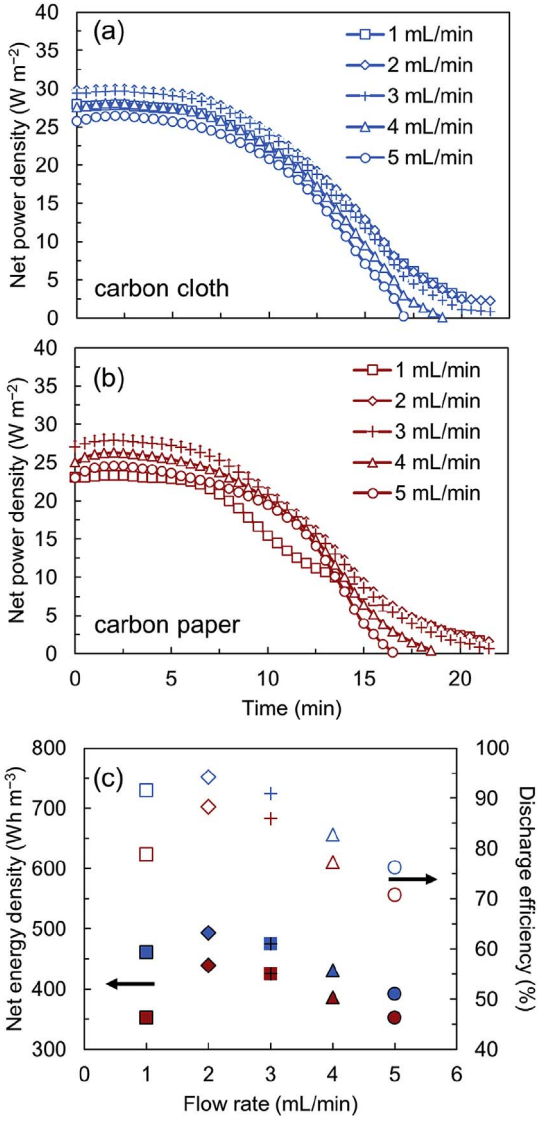

Fig. 6. Net power production over one cycle of the flow silver TRAB with (a) carbon cloth and (b) carbon paper based Ag electrodeposited electrodes. (c) Discharge efficiency (open symbols) and net energy (filled symbols) produced during the operation of the cell at different flow rates. The initial electrolyte contained 0.1 M $AgNO_3$, 5 M NH_4NO_3 as the supporting electrolyte and additional 2 M NH_4OH in the anolyte.

cloth and paper are suitable electrode substrates for Ag-TRAB.

3.2.5. Reversibility over successive cycles

Since the Ag-TRAB would need to be operated over many successive closed-loop cycles, in which the electrodes alternatively function as cathodes and anodes, cell cyclability was examined over 100 cycles (Fig. 8, Fig. S7). Cell potentials and power production were stable, indicating excellent reversibility of the silver deposition and dissolution reactions on the electrodes. Previous TRAB systems failed to operate after just a few cycles (less than 10 cycles) [18,20], while here the system showed no change in performance even after 100 cycles. While conventional batteries are often tested for thousands of cycles, flow batteries (which are more similar to the system developed here) are typically only tested for a hundred of cycles (usually 10–100 cycles) [37–40]. Examination of the electrodes after 100 cycles using SEM showed an absence of particle agglomeration of silver particles on the carbon materials. The carbon substrate also showed no evidence of any physical degradation, confirming the high stability of the substrate under the discharge condition. The average particle size of the deposited silver also did not appreciably change over the cycles (Fig. S8).

4. Outlook

The flow silver-based TRAB developed here demonstrated very stable cycling performance which is needed for systems to convert waste heat to electricity. Due to the optimized design of the battery, the volumetric power density was increased to 125 kW m^{-3} (compared to 15 kW m^{-3} for previous copper based TRAB) [19], based on the total reactor working volume. The energy efficiency relative to the Carnot efficiency (3.8%) was also in a range that could enable the system to be commercially viable. These characteristics for stability, power density, and efficiency, suggest that the technology could be a viable approach to convert low-grade waste heat to electricity.

An important factor for further development of Ag-TRAB is the cost of the materials relative to energy production. In order to be commercially viable, the price of electricity produced by this technology should be competitive with prices for other alternative and conventional electrical power methods. Based on commercial prices of the main materials for the Ag-TRAB (carbon paper, the AEM membrane, silver nitrate, ammonium nitrate, ammonia, and the reactor body), the price of the energy produced was estimated to be $220 per MWh, not considering any costs for waste heat. This is 57% higher than average current electricity prices of alternative electrical power production technologies (e.g., solar, wind, geothermal, etc.) (Fig. S9, Fig. S10). A major cost of the TRAB is the ion exchange membrane (~48% of the

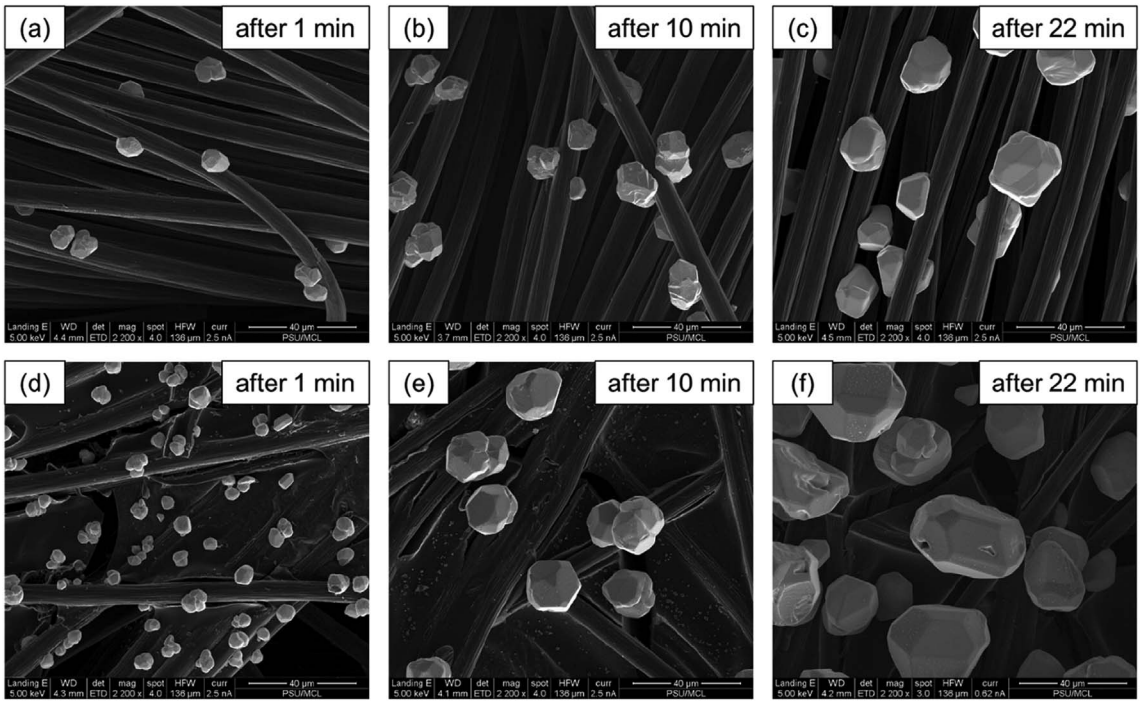

Fig. 7. Investigation on the electrode behavior during the battery discharge using SEM analysis. SEM images of the silver electrodeposited cathode with (a, b, c) carbon cloth and (d, e, f) carbon paper substrates after certain discharge times (labeled in Fig. 1 min, 10 min, and 22 min).

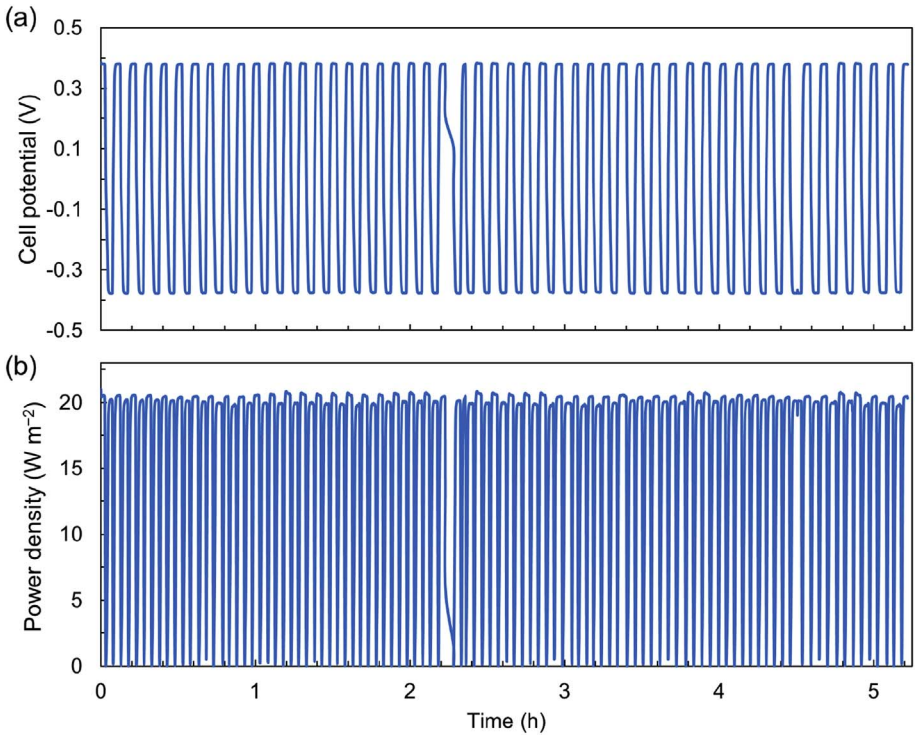

Fig. 8. (a) Cell potential and (b) power production of the silver TRAB with carbon cloth based Ag electrodeposited electrodes for 100 successive cycles. The cell was operated at a hydraulic retention time of 4 s, and the anolyte and catholyte flow path were exchanged every 3 min. An electrolyte with 0.1 M $AgNO_3$, 5 M NH_4NO_3 and 2 M NH_4OH (just for anolyte) was used.

total cost). If the membrane cost could be reduced from \$100 m^{-2} to \$10 m^{-2}, the electricity cost would be improved to \$120 per MWh, making it more competitive with current market prices of electricity based on renewable energy. To make this economic analysis more comprehensive, the cost of the ammonia separation system, as well as the costs of pumps, reservoirs, connections, and operation costs would need to be added to the current economic analysis.

The estimated price of electricity for the Ag-TRAB is 1.8 times more than the average electricity price is the U.S. (\$120 per MWh), which is mostly produced by conventional technologies (i.e., fossil fuels) (Fig. S10). Other potential benefits, such as no air pollution with power generation, and beneficial issues related to health and climate change, were not included in the analysis [41–43]. Although the cost of building and operation relative to energy production of Ag-TRAB is currently higher than that of conventional technologies, this approach could generate a cleaner method of electrical power generation using waste source if the commercial cost of ion exchange membranes could be significantly reduced.

5. Conclusions

A thermally regenerative flow battery based on the use of silver electrodeposited on carbon electrodes was successfully developed here to convert low-grade waste heat to electricity over successive cycles. A net power density of ~ 30 W m^{-2} with a net energy density of ~ 500 Wh m^{-3} was produced by a single cell, operated at a hydraulic retention time of 2 s (flow rate = 2 mL min^{-1}). The Ag-TRAB also showed a very stable power production over a hundred successive cycles. The developed system overcomes the major limitation of the previous cooper-based system of limited reversibility. Considering the power production, stability and reversibility, and the economic aspects, Ag-TRAB could be a promising sustainable approach for electrical power production from low-grade waste heat.

Acknowledgments

The authors would like to thank Julie Anderson, Materials Research Institute (MRI) at Penn State University, for running the SEM and EDS tests. We also acknowledge Prof. Michael Hickner for useful discussions. The research was supported by the National Science Foundation (NSF) through awards CBET-1464891 and CBET-1603635, and Penn State University.

Appendix A. Supplementary data

Supplementary data related to this article can be found at http://dx.doi.org/10.1016/j.jpowsour.2017.10.089.

References

[1] L.E. Bell, Science 321 (2008) 1457–1461.
[2] K. Biswas, J. He, I.D. Blum, C.-I. Wu, T.P. Hogan, D.N. Seidman, V.P. Dravid, M.G. Kanatzidis, Nature 489 (2012) 414–418.
[3] S. Tavakkoli, O.R. Lokare, R.D. Vidic, V. Khanna, ACS Sustain. Chem. Eng. 4 (2016) 3618–3626.
[4] International Energy Agency Energy Policies of IEA Countries the United States 2014 Review vol 40 (2014).
[5] A.P. Straub, N.Y. Yip, S. Lin, J. Lee, M. Elimelech, Nat. Energy 1 (2016) 16090.
[6] A. Carati, M. Marino, D. Brogioli, Energy 93 (2015) 984–993.
[7] O.R. Lokare, S. Tavakkoli, G. Rodriguez, V. Khanna, R.D. Vidic, Desalination 413 (2017) 144–153.
[8] T. Kim, M. Rahimi, B.E. Logan, C.A. Gorski, ChemSusChem 9 (2016) 981–988.
[9] E. Mostavi, S. Asadi, D. Boussaa, Energy 121 (2017) 606–615.
[10] S. Chu, A. Majumdar, Nature 488 (2012) 294–303.
[11] F. Hao, P. Qiu, Y. Tang, S. Bai, T. Xing, H.-S. Chu, Q. Zhang, P. Lu, T. Zhang, D. Ren, J. Chen, X. Shi, L. Chen, Energy Environ. Sci. 9 (2016) 3120–3127.
[12] T.J. Salez, B.T. Huang, M. Rietjens, M. Bonetti, C. Wiertel-Gasquet, M. Roger, C.L. Filomeno, E. Dubois, R. Perzynski, S. Nakamae, Can charged colloidal particles increase the thermoelectric energy conversion efficiency? Phys. Chem. Chem. Phys. 19 (14) (2017) 9409–9416.
[13] R. Hu, B.A. Cola, N. Haram, J.N. Barisci, S. Lee, S. Stoughton, G. Wallace, C. Too, M. Thomas, A. Gestos, M.E.d. Cruz, J.P. Ferraris, A.A. Zakhidov, R.H. Baughman, Nano Lett. 10 (2010) 838–846.
[14] T.J. Abraham, D.R. MacFarlane, J.M. Pringle, Energy Environ. Sci. 6 (2013) 2639–2645.
[15] H. Im, T. Kim, H. Song, J. Choi, J.S. Park, R. Ovalle-Robles, H.D. Yang, K.D. Kihm, R.H. Baughman, H.H. Lee, T.J. Kang, Y.H. Kim, Nat. Commun. 7 (2016).
[16] L. Zhang, T. Kim, N. Li, T.J. Kang, J. Chen, J.M. Pringle, M. Zhang, A.H. Kazim, S. Fang, C. Haines, D. Al-Masri, B.A. Cola, J.M. Razal, J. Di, S. Beirne, D.R. MacFarlane, A. Gonzalez-Martin, S. Mathew, Y.H. Kim, G. Wallace, R.H. Baughman, Adv. Mater 29 (2017) 1605652-n/a.
[17] A. Gunawan, C.-H. Lin, D.A. Buttry, V. Mujica, R.A. Taylor, R.S. Prasher, P.E. Phelan, Nanosc. Microsc. Therm. 17 (2013) 304–323.
[18] F. Zhang, J. Liu, W. Yang, B.E. Logan, Energy Env. Sci. 8 (2015) 343–349.
[19] X. Zhu, M. Rahimi, C.A. Gorski, B. Logan, Chem. Sus. Chem 9 (2016) 873–879.
[20] F. Zhang, N. LaBarge, W. Yang, J. Liu, B.E. Logan, Chem. Sus. Chem 8 (2015) 1043–1048.
[21] M. Rahimi, A. D'Angelo, C.A. Gorski, O. Scialdone, B.E. Logan, J. Power Sources 351 (2017) 45–50.
[22] A.J. Bard, R. Parsons, J. Jordan, Standard Potentials in Aqueous Solution, Taylor & Francis, 1985.
[23] M. Rahimi, L. Zhu, K.L. Kowalski, X. Zhu, C.A. Gorski, M.A. Hickner, B.E. Logan, J. Power Sources 342 (2017) 956–963.
[24] W. Zhao, Z. Xu, T. Sun, S. Liu, X. Wu, Z. Ma, J. He, C. Chen, J. Alloys Compd. 584 (2014) 635–639.
[25] A. Afkhami, T. Madrakian, Z. Karimi, J. Hazard. Mater 144 (2007) 427–431.
[26] M. Rahimi, Z. Schoener, X. Zhu, F. Zhang, C.A. Gorski, B.E. Logan, J. Hazard. Mater 322 (2017) 551–556.
[27] T. Kim, M. Rahimi, B.E. Logan, C.A. Gorski, Environ. Sci. Technol. 50 (2016) 9791–9797.
[28] T. Kim, B.E. Logan, C.A. Gorski, Energy Environ. Sci. 10 (2017) 1003–1012.
[29] X. Zhu, W. He, B.E. Logan, J. Membr. Sci. 486 (2015) 215–221.
[30] J. Veerman, M. Saakes, S.J. Metz, G.J. Harmsen, Environ. Sci. Technol. 44 (2010) 9207–9212.
[31] D.A. Vermaas, M. Saakes, K. Nijmeijer, Environ. Sci. Technol. 45 (2011) 7089–7095.
[32] X. Zhu, T. Kim, M. Rahimi, C.A. Gorski, B.E. Logan, ChemSusChem 10 (2017) 797–803.
[33] A. El-kharouf, T.J. Mason, D.J. Brett, B.G. Pollet, J. Power Sources 218 (2012) 393–404.
[34] C. Qin, J. Electrochem. Soc. 162 (2015) F1036–F1046.
[35] L. Cindrella, A. Kannan, J. Lin, K. Saminathan, Y. Ho, C. Lin, J. Wertz, J. Power Sources 194 (2009) 146–160.
[36] T.I. Quickenden, Y. Mua, J. Electrochem. Soc. 142 (1995) 3985–3994.
[37] B. Huskinson, M.P. Marshak, C. Suh, S. Er, M.R. Gerhardt, C.J. Galvin, X. Chen, A. Aspuru-Guzik, R.G. Gordon, M.J. Aziz, Nature 505 (2014) 195–198.
[38] W. Wang, Q. Luo, B. Li, X. Wei, L. Li, Z. Yang, Adv. Funct. Mater 23 (2013) 970–986.
[39] J.D. Milshtein, S.L. Fisher, T.M. Breault, L.T. Thompson, F.R. Brushett, ChemSusChem 10 (2017) 2080–2088.
[40] M.S. Cha, H.Y. Jeong, H.Y. Shin, S.H. Hong, T.-H. Kim, S.-G. Oh, J.Y. Lee, Y.T. Hong, J. Power Sources 363 (2017) 78–86.
[41] J. Hill, E. Nelson, D. Tilman, S. Polasky, D. Tiffany, Proc. Natl. Acad. Sci. U. S. A. 103 (2006) 11206–11210.
[42] E. Mahdinia, A. Demirci, A. Berenjian, World J. Microbiol. Biotechnol. 33 (2017) 2.
[43] R. Banos, F. Manzano-Agugliaro, F.G. Montoya, C. Gil, A. Alcayde, J. Gomez, Renew. Sust. Energ. Rev. 15 (2011) 1753–1766.